



Published in final edited form as:

*Metallomics*. 2016 April 1; 8(4): 412–421. doi:10.1039/c6mt00003g.

## Combinatorial phenotypic screen uncovers unrecognized family of extended thiourea inhibitors with copper-dependent anti-Staphylococcal activity

Alex G. Dalecki<sup>1</sup>, Aruni P. Malalasekera<sup>2</sup>, Kaitlyn Schaaf<sup>1</sup>, Olaf Kutsch<sup>1</sup>, Stefan H. Bossmann<sup>2</sup>, and Frank Wolschendorf<sup>1,#</sup>

<sup>1</sup>Department of Medicine, University of Alabama at Birmingham, Birmingham, AL, USA

<sup>2</sup>Department of Chemistry, Kansas State University, Manhattan, KS, USA

### Abstract

The continuous rise of multi-drug resistant pathogenic bacteria has become a significant challenge for the health care system. In particular, novel drugs to treat infections of methicillin-resistant *Staphylococcus aureus* strains (MRSA) are needed, but traditional drug discovery campaigns have largely failed to deliver clinically suitable antibiotics. More than simply new drugs, new drug discovery approaches are needed to combat bacterial resistance. The recently described phenomenon of copper-dependent inhibitors has galvanized research exploring the use of metal-coordinating molecules to harness copper's natural antibacterial properties for therapeutic purposes. Here, we describe the results of the first concerted screening effort to identify copper-dependent inhibitors of *Staphylococcus aureus*. A standard library of 10,000 compounds was assayed for anti-staphylococcal activity, with hits defined as those compounds with a strict copper-dependent inhibitory activity. A total of 53 copper-dependent hit molecules were uncovered, similar to the copper independent hit rate of a traditionally executed campaign conducted in parallel on the same library. Most prominent was a hit family with an extended thiourea core structure, termed the NNSN motif. This motif resulted in copper-dependent and copper-specific *S. aureus* inhibition, while simultaneously being well tolerated by eukaryotic cells. Importantly, we could demonstrate that copper binding by the NNSN motif is highly unusual and likely responsible for the promising biological qualities of these compounds. A subsequent chemoinformatic meta-analysis of the ChEMBL chemical database confirmed the NNSNs as an unrecognized staphylococcal inhibitor, despite the family's presence in many chemical screening libraries. Thus, our copper-biased screen has proven able to discover inhibitors within previously screened libraries, offering a mechanism to reinvigorate exhausted molecular collections.

### INTRODUCTION

The advent of high throughput screening (HTS) technologies over thirty years ago revolutionized drug discovery efforts. Having apparently exhausted the readily identifiable repertoire of natural antibacterials derived from soil bacteria, HTS strategies began a

<sup>#</sup>corresponding author: Frank Wolschendorf, Department of Medicine, University of Alabama at Birmingham, 845 19<sup>th</sup> Street S, Birmingham, AL 35294, fwolsche@uab.edu, Phone: 1-205-975-2760.

renaissance in drug discovery, promising an effectively unlimited supply of novel compounds to combat the emerging threat of antibiotic resistance<sup>1</sup>. However, despite ever-expanding compound libraries and highly efficient screening methodologies, new classes of synthetic antibiotics have yet to materialize. The increasing concerns of returning to a pre-antibiotic era have proven severe enough to warrant attention and action by top governmental agencies<sup>2, 3</sup>.

Of the sixteen antibiotic classes used clinically, all but two were derived from environmental sources, and there is growing interest in returning to natural inspirations<sup>1, 4-6</sup>. Among these inspirations lies metal-mediated innate immunity, by which the innate immune system directly modulates environmental levels of metals such as manganese, iron, zinc, and copper at the site of infection<sup>7, 8</sup>. Through limitation, in the case of iron, zinc, and manganese or oversaturation, in the case of copper, the intrinsic properties of these ions are utilized to form a crucial line of defense against pathogens. Growing bodies of evidence point toward copper's essentiality in particular. In many systems, including *Mycobacterium tuberculosis*, *Pseudomonas aeruginosa*, *Listeria monocytogenes*, and *Streptococcus pneumoniae*, bacterial copper resistance is linked to virulence<sup>9</sup>; conversely, attenuation of the "copper burst" within macrophages weakens the phagocytic response, promoting bacterial survival<sup>10, 11</sup>. All sequenced bacteria possess at least a rudimentary level of copper resistance machinery<sup>12</sup>, varying from simple expression of an efflux pump<sup>13</sup>, to a complex network including pumps, sequestration proteins, oxidases, chaperones, and transcriptional regulators<sup>14</sup>. As free copper levels are buffered below one ion per cell in both prokaryotes<sup>15</sup> and eukaryotes<sup>16</sup>, that even obligate intracellular bacteria retain resistance machinery further underscores copper's profound role as an environmental and immunological insult<sup>12</sup>.

Recent advances in our understanding of copper's role in immunity have paralleled the rise of reports detailing the phenomenon of copper-dependent antibiotics. These compounds are highly inhibitory in the presence of copper, yet impotent in its absence. Example inhibitors have been described for Gram negatives<sup>17</sup>, Gram positives<sup>18</sup>, and mycobacteria<sup>19</sup>, as well as eukaryotic targets including pathogenic fungi<sup>20</sup> and cancer cells<sup>21-23</sup>. The broad range of potential targetable pathogens, coupled with the wide array of novel mechanisms of action, has generated interest in exploiting copper's antibiotic properties<sup>24, 25</sup>. However, until now, discoveries have been largely serendipitous, or based upon established metal-binding motifs; though well suited for chemical probes, these scaffolds are often poorly adaptable to therapeutic uses. Exploring the full potential of copper-mediated therapeutics requires new motifs and a directed discovery effort to identify proof-of-principle compounds.

Here, we demonstrate for the first time the power of a copper-focused HTS screening campaign. This approach is uniquely able to uncover new interactions between copper ions and compounds in existing chemical libraries, and their subsequent synergistic inhibitory activities. A copper-biased combinatorial screen against *Staphylococcus aureus* revealed nearly twice as many hits as a traditional, copper-blind campaign. A reoccurring extended thiourea motif, dubbed NNSN, featured novel copper-binding properties, and was revealed by UV/Vis and NMR analysis to participate in a new interaction between the ligand and copper ion. This motif was highly inhibitory against *S. aureus* in a copper-dependent and copper-specific manner, yet was well tolerated in cell culture. Finally, despite their presence

in many screening libraries, a chemoinformatic meta-analysis demonstrated NNSNs as previously unrecognized antistaphylococcal agents, confirming the ability of copper-biased screens to discover new compounds hiding in existing chemical space.

## METHODS

### Bacterial strains, antibiotics and compounds

*S. aureus* clinical isolate SA3 (resistant to ampicillin, clindamycin, erythromycin, penicillin, and tetracycline) was characterized by and obtained in a de-identified manner from UAB Laboratory Medicine. Bacteria were routinely grown in Mueller Hinton (MH) medium (Oxoid Ltd., Basingstoke, Hampshire, England) overnight at 37°C before inoculating plates according to assay conditions unless otherwise stated. All experiments were performed in 96-well plates using MH medium or RPMI1640 medium supplemented with trace metals. The trace metal mix was prepared as a 1,000-fold stock solution containing 3mM EDTA, 50mM MgCl<sub>2</sub>, 0.7 mM CaCl<sub>2</sub>, 80µM NaMoO<sub>4</sub>, 168 µM CoCl<sub>2</sub>, 0.55 mM MnCl<sub>2</sub>, 0.7 mM ZnSO<sub>4</sub>, 2 mM FeSO<sub>4</sub>. All screened compounds were randomly taken from our 43,000 in-house compound library (Chembridge) or Chembridge's Hit2Lead online library ([www.hit2lead.com](http://www.hit2lead.com)). Copper sulfate and all other commercial compounds were purchased from Sigma-Aldrich. Copper treated assays were supplemented with 50 µM CuSO<sub>4</sub> unless otherwise indicated. Other metals were used at 100 µM or as indicated.

### High throughput screening assay

The HTS assay was conducted as published previously<sup>18</sup>. Briefly, all compounds were screened at 10 µM in duplicate plates run in parallel, one containing only medium (trace-copper conditions) and one containing medium supplemented with 50 µM CuSO<sub>4</sub>. *S. aureus* was added to each well to achieve a final optical density (OD<sub>600</sub>) of ~0.001 to 0.004 (1:1000 dilution of an overnight culture) in a total volume of 160 µl. All steps were performed using the Precision Power automated microplate pipetting system (BioTek). Plates were sealed with parafilm (Millipore) to minimize evaporation and incubated on a Heidolph Titramax 1000 plate shaker at 450 rpm at 37°C for 8 hours. Optical density, as a quantitative surrogate marker of bacterial growth, was determined using a Synergy HT plate reader (BioTek). Background correction was performed against wells containing only medium and compounds that decreased the growth of *S. aureus* were identified and further analyzed.

### HTS data analysis

An in-house algorithm was utilized for analysis. The software package used MySQL and PHP as a server backend, and a web accessible HTML interface as the front end. Hits were defined based upon number of standard deviations (1 SD = 20%) from the overall mean, which averaged 94% across all copper-replete samples after blank correction and normalization to positive controls. Independent hits were compounds with less than 34% growth (3 SDs from the mean) in both standard and copper supplemented conditions. Copper dependent hits had under 34% growth in the copper replete plate, with at least 40 percentage points (2 SD) more growth in copper trace plates (*e.g.*, 20% growth in Cu-replete and >60% growth in Cu-trace plates). Inverse hits were the opposite, with under 34% growth in trace plates and at least 40 percentage points more growth in replete plates. Substructure

analysis was completed using the Open Babel 2.3.2 chemistry toolbox, as installed on a Linux server<sup>26</sup>. The SMARTS search string for non-cyclic thioureas was “[N;!R]C(=S)[N;!R],” while the NNSN substructure search was extended to “[#7][#6][N;!R]C(=S)[N;!R]” to include both cyclic and non-cyclic carbons and nitrogens.

### Structure Activity Relationship (SAR) Studies (SAR-by-catalogue)

Active molecules were grouped based on the occurrence of structural motifs identified during visual and computational inspection of their chemical structures. Representative compounds and additional derivatives of each group were ordered from [www.hit2lead.com](http://www.hit2lead.com). Activity was confirmed in dose response curves, of which we also determined the MIC (for details see below). Additional compounds featuring respective key motifs were identified in the Chembridge Hit2Lead online library using the search feature provided on the website ([www.hit2lead.com](http://www.hit2lead.com)).

### Determination of the minimal inhibitory concentration (MIC)

Compounds were reconstituted in sterile DMSO (Sigma-Aldrich) typically at a concentration of 10 mM, then aliquotted, and stored at  $-80^{\circ}\text{C}$ . In some instances, a decline in potency of the compounds was noted over a period of 6 months and after repeatedly freezing and thawing reconstituted compounds. Compounds were diluted in 96-well in 2-fold increments, typically covering a concentration range from  $\sim 0.07$  to 10  $\mu\text{M}$ . Control wells containing media only (sterility control) and media with cells in the absence of compound with or without 50  $\mu\text{M}$  copper were included as well. Assay conditions and incubation procedure were similar to that of the pilot screen. Dose-response curves were analyzed by determining the  $\text{OD}_{600}$  using a plate reader (Synergy HT, BioTek). Data was analyzed as the average value of 3 wells with identical conditions and normalized to the proper growth controls. MIC was defined as the concentration at which growth was reduced by at least 85%. Additional transition metals were assayed in Roswell Park Memorial Institute 1640 medium without phenol red (RPMI; Life Technologies) and supplemented with a 1:1000 dilution of a copper-free trace metal mix (RPMI1640+TM) to promote growth<sup>27</sup>.

### Eukaryotic toxicity assessment

THP-1 cells were grown in standard RPMI plus 10% FBS. Cells were plated in RPMI at 100,000 cells per well in a total volume of 200  $\mu\text{L}$  in a 96 well plate, and challenged with compound in the presence or absence of 15  $\mu\text{M}$  Cu for 24 hours. This copper concentration was well tolerated by THP-1 cells in our system and lies within the physiological range of copper levels in blood (10–25  $\mu\text{M}$ )<sup>28</sup>. Viability was read using a Guava flow cytometer, through gating on live populations as assessed through forward and side scatter measurements.

### Characterization of metal complexation and structure modeling

The binding constants of CuBr in Trizma-HCl (pH=7)/methanol (90/10 v/v) to compounds were determined according to the method of Benesi and Hildebrand<sup>29</sup>. The binding of Cu(II) and Cu(I) enhances the UV-absorption band of APT-6i at  $\lambda_{\text{max}} = 235\text{nm}$ . The differences in

UV-absorption at  $\lambda_{\max} = 235\text{nm}$  were used to calculate the binding constants  $K_B$ . UV/Vis spectra of 8.3, 17, 41, 83, 170 and 410 nM of APT-6i were recorded in the absence and presence of 10  $\mu\text{M}$  CuBr (Sigma-Aldrich, ACS grade) at 283 K in Trizma-HCl (pH=7.0)/methanol (1:1 v/v) using a Varian Cary 500 UV/Vis-NIR spectrophotometer and 4.0 mL quartz cuvettes. The measurements were performed under argon to avoid Cu(I) oxidation to Cu(II).

### NMR Titrations

$^1\text{H}$ -NMR spectra were recorded using a Bruker Avance III, 600 MHz NMR-spectrometer at 298K. Compound APT-6i was dissolved in deuterated acetone (6.25 mM), total volume: 400  $\mu\text{l}$ . Cu(I) was added from a stock solution of  $1.5 \times 10^{-4}$  M CuBr in deuterated acetone. 5 mL of  $\text{CH}_3\text{OD}$  was added as internal standard (peak not shown).

### ChEMBL database meta-analysis

The ChEMBLdb relational database, version 20, was downloaded as the provided virtual machine (MyChEMBL)<sup>30, 31</sup>. All SQL searches were conducted from a Linux command line interface.

## RESULTS

### Copper-biased HTS environment uncovers numerous copper-dependent hits

**(1) Nearly twice as many hits discovered through copper-biased screen as in a traditional screen**—Metal-based antibiotics have not yet advanced to clinical or veterinarian use and are therefore an attractive alternative to conventional antibiotics. Surprisingly, high throughput screening (HTS) solutions for the discovery of novel metal-related antibacterial activities do not exist. We focused our screen on compounds that display antibacterial properties through the interaction of copper because of its potential physiological relevance in the context of copper-mediated innate immune functions<sup>7, 24</sup>, competitiveness over other physiological metal ions<sup>32</sup>, and intrinsic antibacterial properties<sup>33</sup>. To reveal novel copper binding compounds not active in the absence of copper, we conducted a parallel screen, in which compounds were tested both under standard, traditional conditions, as well as in the presence of copper (Figure 1). This strategy allowed us to comprehensively determine the spectrum of effects that copper ions might have on the antibacterial properties of potential bacterial inhibitors with copper-related activities (enhancing or mitigating). Screening only in the presence of copper and testing only hits for their activity in the absences of copper would have missed a group of compounds that we classify as inverse hits. We chose to screen at 50  $\mu\text{M}$  copper to enable detection of compounds with weaker copper-dependent activity (classified as secondary and tertiary hits), in order to better inform SAR, hit cluster expansion, and hit prioritization strategies.

Screening our 10,000 compound test library against a clinically isolated drug-resistant *S. aureus* strain (SA3) identified 129 total hits, or 1.29% of the overall number of compounds. Comparison of the hits from both the trace-copper screen (Figure 2A) and copper-supplemented screen (Figure 2B) revealed 70 compounds (54%) that were similarly inhibitory under both screening conditions (copper independent hits) and 6 compounds (5%)

that lost their antibacterial properties in the presence of copper (copper inverse hits). Importantly, 53 molecules (41%) were found only in the presence of copper, demonstrating that copper-activated antibacterial activities occur rather frequently. Of the copper-dependent hits, over half (28) met our criteria for a primary hit, *i.e.*, more than 90% inhibition. These copper-dependent hits represent hitherto unrecognized inhibitors, given that conventional screening campaigns for antibiotics do not contain sufficient and physiological quantities of copper ions.

**(2) Copper-dependent hits display significantly different chemical properties compared to the library as a whole**—Unfortunately, there is often a great disparity between molecules with desirable activities and molecules that are “druggable”. To concentrate discovery efforts on promising compounds, certain guidelines such as Lipinski’s Rule of Five (Ro5) have been developed<sup>34, 35</sup>. Originally, these guidelines described four rules: molecular weights (MW) < 500 Da, octanol/water partition coefficient (cLogP) < 5, hydrogen bond donors < 5, and hydrogen bond acceptors < 10. The criteria were later extended to include topological polar surface area (tPSA) < 140 Å<sup>2</sup> and rotational bonds (RB) < 10. To visualize our results in aggregate, we compared Ro5 values of dependent hits, independent hits, inverse hits, and the screened library as a whole. Molecular weight only varied slightly between groups, and all were statistically indistinguishable from the library as a whole (Figure 3A). Rotational bonds and cLogP values were slightly significantly different when comparing copper-dependent hits to the screened library ( $p = 0.0122$  and  $0.0116$ , respectively), though all three categories clustered toward the top of the cLogP and bottom of the RB ranges (Figures 3B, 3C). Topological polar surface area (tPSA) differed greatly between dependent hits and all other categories ( $p < 0.0001$ ), with the dependent hit median tPSA 38% lower than the library average (Figure 3D). The most striking comparison, however, came from numbers of hydrogen bond donors and acceptors. The screened library had a relatively even distribution of both acceptors and donors (Figure 3E), with a median of 4 acceptors and 1 donor; while the median of copper-dependent hits clustered tightly at only 1 acceptor and 2 donors (Figure 3G). These structural differences may enable assembly or construction of custom libraries targeted towards enhanced copper-binding molecules.

### Extended thiourea structure comprised a well-established hit cluster

**(1) Novel NNSN motif associated with copper-dependent antistaphylococcal activity**—While our data indicates that the presence of physiologically relevant trace elements, specifically copper, reveals new hit molecules within a given compound collection, it is also important to demonstrate that the identified hits found by this alternative method are functionally relevant and responsive to optimizations. To substantiate this, we began a substructure analysis of our copper-dependent hits with the goal to identify repeatedly occurring chemical motifs and use such motifs as starting points for future SAR analysis. Thioureas (Figure 4A) dominated our copper-dependent hits, comprising 45 of the 53 total hits, or 85%. Such a high proportion greatly contrasted with the library as a whole, which featured only 570 thioureas in total (5.7%). Further, thioureas were not found to be generally active but rather possessed a specific copper-dependent activity, as only 7 of the 70 copper-independent hits contained a thiourea motif. This fraction was not significantly

different in proportion from the entire library as judged by a chi-squared analysis ( $p=0.119$ ). Thus, not only did the screening conditions appear to have enriched our results specifically for the thiourea motif, but also have identified thioureas as the first example of a discrete chemical substructure identified by HTS that possesses strictly metal-dependent antibacterial activities.

Interestingly, 12 of the 45 thioureas featured an extended thiourea structure, which we dubbed NNSN-motif (Figure 4B). No NNSN-motif was found among the copper-independent hits. All 12 copper-dependent NNSN molecules featured a linear thiourea structure, complemented by a heterocyclic ring system (pyrazolyl, tetrazolyl, thiazolyl, pyridinyl, pyrimidinyl or pyrazinyl) to form the full NNSN motif (Figure 4C). Molecular flexibility appeared to be essential for activity since rigid NNSN motifs with a cyclic thiourea structure as in triazolethiones (Figure 4D), imidazo-pyrimidine-thiones (Figure 4E) or pyrido-pyrimidine-thiones (Figure 4F) were inactive. A substructure search within the structures of all 10,000 randomly picked molecules that were included in our screen identified 30 total non-cyclic NNSN motifs; thus, the screen discovered 40% of all possible NNSN molecules.

## **(2) Adamantyl-bearing pyrazolyl-thioureas (APTs) yielded fruitful structure activity relationship analysis**

—In order to probe whether NNSN-compounds have the potential of being further developed towards early lead status, we conducted a limited structure activity relationship study on 9 commercially available pyrazolyl-thiourea derivatives featuring an adamantyl group (Figure 5). Adamantyl bearing pyrazolyl-thioureas (APTs) were chosen because adamantyl substituents are known to improve drug stability and plasma half-life by impeding the access of hydrolytic enzymes through restricting or altering intramolecular reactivity<sup>36</sup>, and because adamantyl groups have no significant reactivity allowing us to link activity differentials to other substituents<sup>36</sup>. No activity was observed in medium without copper for any of these molecules, but in copper-supplemented medium the compounds had minimum inhibitory concentrations (MICs) between 0.3 and 10  $\mu\text{M}$  (Figure 5).

Among the analogs tested, APT-6i (Figure 4G) exhibited excellent copper-dependent inhibition of *S. aureus* (Figure 6A), with a minimum inhibitory concentration of 0.3  $\mu\text{M}$ . Additionally, APT-6i was relatively benign toward THP-1 cells, a human monocyte cell line (Figure 6A). Activity was also entirely copper-specific, with no observed inhibition when growth media was supplemented with other transition metals such as Mn, Fe, Co and Zn (Figure 6B). However, the presence of additional metals did not preclude activity, as full inhibition was restored upon co-incubation of Zn and Cu with APT-6i (Figure 6B).

## **Pyrazolyl-thioureas are functionalized through unique copper-coordination chemistry**

To further examine the interaction between APT-6i and copper, we analyzed the metal-ligand complex using UV-Vis spectroscopy and <sup>1</sup>H-NMR. UV-Vis titrations are a straightforward method to visualize metal-ligand complex formation, and revealed a main absorption peak at  $\lambda=235$  nm, with intensity strongly dependent on the APT-6i concentration (Figure 7A). This peak represents an energy shift in electron orbitals, indicative of complex

formation and subsequent  $\pi$  bonding between the copper ion and ligand. Further analysis through the Benesi-Hildebrand method<sup>29</sup> produced linear plots, confirming a 1:1 stoichiometry within the ligand-metal complex (Figure 7B). The binding constant of CuBr and APT-6i in Trizma/methanol was calculated to  $K_B = 476,700 \pm 1200$  (L mol<sup>-1</sup>).

As we were unable to obtain crystal structures of the Cu(I) and APT-6i complex, we relied on <sup>1</sup>H-NMR-titration with CuBr in deuterated acetone to discern the structure formed in solution (Figure 7C). Intriguingly, the <sup>1</sup>H-NMR titration confirmed that the observed 1:1 complexation geometry is clearly different from canonical Cu(I)-thiourea complexes, which usually feature at least two thiourea ligands per metal cation. It is especially noteworthy that both thioamide groups, but not the thiocarbonyl group, take part in the observed complexation. Following the shift of peak position 4 from  $\delta=5.931$  to 5.984 ppm with increasing CuBr concentration (Figure 7E), it is apparent that one of the aromatic carbons of the pyrazole unit is in close proximity to Cu(I) in solution, assuming that a CH<sub>3</sub>OD molecule (added as internal standard) is also coordinated to Cu(I) in order to obtain a slightly distorted tetrahedral geometry. The solution structure of the APT-6i-Cu(I) complex is the basis for the molecular modeling (Figure 8A, 8B, 8C). From our modeling, it becomes clear that significant conformational changes are required to accommodate the complexation of a central Cu(I) cation (Figure 8B, 8C).

More importantly to drug discovery efforts, this novel complexation could potentially reopen the door to a wide array of otherwise unattractive compounds. Although thioureas readily complexes metal ions, and are thus logical candidates for discovery by the paradigm detailed here, they are often regarded as undesirable due to common hepatotoxicity and thyroid peroxidase inhibition<sup>37</sup>. Sulfur's lack of participation in the complex suggests the possibility of bioisosteric substitution of other functional groups or atoms, negating toxicity while retaining complexation ability and antibacterial activity. Previous reports offer precedent, though results are expectedly mixed: some substitutions, such as cyanoguanidines, retained activity or increased therapeutic indices<sup>38</sup>, while others lost biological activity<sup>39</sup>. A concerted SAR effort would likely produce new metal-complexing non-thioureas.

### Meta-analysis reveals NNSNs as previously unrecognized antistaphylococcal agents

Having identified the NNSN motif as a promising and novel copper-dependent antibacterial structure, we examined whether this motif had previously been recognized for its therapeutic potential. We conducted a meta-analysis of published activities using the ChEMBL database, a publically available relational database containing over 13 million activity records of 1.4 million compounds, taken from multiple sources including 2700 PubChem BioAssays and tens of thousands of primary literature reports<sup>30</sup>. The database facilitates tracking individual compounds through a large number of systems, such as biochemical assays, whole cell screens, and *in vivo* data, against prokaryotic and eukaryotic targets. Although ChEMBL does not generally include inactive hits, it is a rich repository of bioactive compounds in a variety of contexts.

Querying the NNSN motif against the database returned 608 hits with recorded activity (Figure 9). Narrowing the search to only whole-cell activities against *S. aureus* returned only 57 hits. Most of these activities, however, were pulled from batch synthesis efforts reported



in the literature, rather than from a directed screening campaign. Of the entire set, 39 had reported MICs below 500  $\mu\text{M}$ , and only 5 had MICs below 50  $\mu\text{M}$ ; of these, only a single compound had a MIC below 10  $\mu\text{M}$ <sup>40</sup>. Given that HTS are limited to testing only one concentration, often at 10  $\mu\text{M}$ , it is likely none of these compounds would have been found individually in a screening campaign, and, hence, would not have been identified as a lead series.

## DISCUSSION

In this study, we report the results of the first high throughput screening (HTS) campaign for the discovery of copper-dependent antibacterial inhibitors. This strategy not only resulted in a much greater number of promising hit molecules than traditional screening methods, but also specifically revealed a previously unknown hit series, whose anti-staphylococcal activity escaped previous detection despite being present in many screening libraries.

Though metal complexation screens could hypothetically proceed using any of the first row transition metals (Mn, Fe, Co, Ni, Cu, and Zn), copper offers the most attractive and most viable vehicle for synergistic inhibition. Copper's antimicrobial properties are multifaceted, but ultimately stem from its relative proclivity toward stable ligand complexation when compared to other transition metal ions. This phenomenon is described by the Irving-Williams series, where complex stabilities are their lowest with manganese, increase in periodic fashion until maximum stability at copper, and finally decline at zinc<sup>41</sup>. Functionally, this gives copper a higher affinity for sulfur, oxygen, and nitrogen than any other physiologically relevant transition metal<sup>42</sup>. This affinity, combined with copper's high redox potential, is often exploited in metallo-proteins such as superoxide dismutases or cytochrome c, and as such is key to the normal function of both prokaryotic and eukaryotic cells. However, copper ions in excess readily displace or replace crucial metalloenzyme cofactors, attack vulnerable iron-sulfur clusters, and directly damage accessible amino acid residues<sup>15</sup>. Cumulatively, these effects heavily interfere with cellular function; as a result, all sequenced bacteria possess at least some level of copper resistance<sup>12</sup>.

As an antimicrobial, copper assaults numerous sites within the cell. Many bacteria have had specific targets identified (*e.g.*, dehydratases in *E. coli*<sup>43</sup>, aerobic nucleotide synthesis in *Streptococcus pneumoniae*<sup>44</sup>, and heme biosynthesis in *Neisseria gonorrhoeae*<sup>45</sup>), but outside of general mechanisms such as attacking iron-sulfur clusters in proteins, specific points of failure vary widely from organism to organism. The detected source of toxicity is simply the "weakest link," or first component to fail. It is very likely some copper-dependent inhibitors feature a similar variety of mechanisms, especially if acting through general copper overload (as in the case of 8-Hydroxyquinoline<sup>20</sup>). More targeted compounds may be capable of additional mechanisms as well. GTSM, for example, acts upon the electron transport chain of *N. gonorrhoeae*, with its spectrum of activity hypothesized to be explained through a particular bacterium's reliance on aerobic respiration<sup>17, 25</sup>. Yet, GTSM is also a potent copper-dependent inhibitor of *S. pneumoniae* (<sup>25</sup>; unpublished observations), a facultative anaerobe lacking an electron transport chain. Thus, additional modes of action must be at play, indicating a multi-faceted mechanism of activity. Though the "magic bullet" paradigm of one drug-one target has dominated since its proposal by Paul Ehrlich a century

ago<sup>46</sup>, copper-dependent inhibitors may offer an alternative: since multiple individual targets could be vulnerable, development of resistance would be much more difficult than against traditional, single target antibiotics.

The allure of copper's anti-bacterial properties has not gone unnoticed<sup>17–20, 25, 47–49</sup>. Unfortunately, free copper ions have little therapeutic value due to their erratic reactivity<sup>50–53</sup>. To pharmacologically control the activity of copper ions and direct them to a specific target, numerous chemosynthetic efforts have synthesized copper complexes with greatly enhanced antibacterial activities<sup>47, 54–58</sup>. However, many of these rely on metal binding motifs that had analytical and technical purposes, rather than medicinal applications. Subsequent synthesis efforts often prioritize advancing the frontiers of organo-metallo-chemistry (e.g. mixed ligand complexes), leaving biological considerations as a secondary focus. Consequently, structure activity relationship studies, such as exemplified by the clinically used metalloantibiotic bacitracin<sup>59</sup>, are extremely rare. While powerful in its own right, the agnosticism of this chemosynthetic strategy toward biological considerations impedes its applicability to HTS discovery. Though we have begun exploring how to harness the potential of copper in chelate based metalloantibiotics, we still need HTS solutions to probe the existing chemical space for novel metal-related activities to facilitate discovery and development of innovative metal-oriented therapeutics.

## CONCLUSION

In summation, our work details the first concerted antibiotic HTS discovery effort to harness the activity of an unconventional antimicrobial, copper. These unique inhibitors have, until now, largely gone unnoticed within conventional screening libraries, offering a way to repurpose and reprobe existing chemical collections. Though therapeutically infeasible on its own, copper's potential can be readily exploited through combination with small organic molecules, offering a promising new approach in the battle for novel antibacterials.

## Acknowledgments

The authors would like to thank Saran Kupul for excellent technical assistance and lab management. Some research of this study was supported by the University of Alabama at Birmingham's (UAB) Department of Medicine, the Center for AIDS Research (UAB CFAR) and its Cytometry Core/Joint UAB Flow Cytometry Core which are funded by NIH/NIAID P30 AI027767 and by NIH 5P30 AR048311, and in part by NIH grant RO1 AI104952 to F.W. In addition, S.H.B. thanks the National Science Foundation for supporting this study (DMR-1242765 and CBET-1337438), as well as Kansas State University, Department of Chemistry. The funding agencies had no role in study design, data collection and interpretation, or the decision to submit the work for publication.

## LITERATURE CITED

1. Lewis K. Nature reviews. Drug discovery. 2013; 12:371–387. [PubMed: 23629505]
2. House, TW. 2014. <http://www.whitehouse.gov/the-press-office/2014/09/18/executive-order-combating-antibiotic-resistant-bacteria>
3. CDC. 2013. <http://www.cdc.gov/drugresistance/pdf/ar-threats-2013-508.pdf>
4. Fischbach MA, Walsh CT. Science. 2009; 325:1089–1093. [PubMed: 19713519]
5. Clardy J, Fischbach MA, Walsh CT. Nature biotechnology. 2006; 24:1541–1550.
6. Demain AL. Nature biotechnology. 2002; 20:331.
7. Hood MI, Skaar EP. Nature reviews. Microbiology. 2012; 10:525–537. [PubMed: 22796883]
8. Fu Y, Chang FM, Giedroc DP. Accounts of chemical research. 2014

9. Hodgkinson V, Petris MJ. The Journal of biological chemistry. 2012; 287:13549–13555. [PubMed: 22389498]
10. White C, Kambe T, Fulcher YG, Sachdev SW, Bush AI, Fritsche K, Lee J, Quinn TP, Petris MJ. Journal of cell science. 2009; 122:1315–1321. [PubMed: 19351718]
11. Johnson MDL, Kehl-Fie TE, Klein R, Kelly J, Burnham C, Mann B, Rosch JW. Infection and immunity. 2015
12. Solioz M, Abicht HK, Mermod M, Mancini S. Journal of biological inorganic chemistry : JBIC : a publication of the Society of Biological Inorganic Chemistry. 2010; 15:3–14. [PubMed: 19774401]
13. Djoko KY, Franiek JA, Edwards JL, Falsetta ML, Kidd SP, Potter AJ, Chen NH, Apicella MA, Jennings MP, McEwan AG. Infection and immunity. 2012; 80:1065–1071. [PubMed: 22184419]
14. Shi X, Darwin KH. Metallomics : integrated biometal science. 2015
15. Foster AW, Osman D, Robinson NJ. Journal of Biological Chemistry. 2014; 289:28095–28103. [PubMed: 25160626]
16. Rae TD, Schmidt PJ, Pufahl RA, Culotta VC, O'Halloran TV. Science. 1999; 284:805–808. [PubMed: 10221913]
17. Djoko KY, Paterson BM, Donnelly PS, McEwan AG. Metallomics : integrated biometal science. 2014
18. Haeili M, Moore C, Davis CJC, Cochran JB, Shah S, Shrestha TB, Zhang Y, Bossmann SH, Benjamin WH, Kutsch O, Wolschendorf F. Antimicrobial agents and chemotherapy. 2014; 58:3727–3736. [PubMed: 24752262]
19. Dalecki AG, Haeili M, Shah S, Speer A, Niederweis M, Kutsch O, Wolschendorf F. Antimicrobial agents and chemotherapy. 2015
20. Festa RA, Hesel ME, Franz KJ, Thiele DJ. Chemistry & biology. 2014; 21:977–987. [PubMed: 25088681]
21. Hadi SM, Ullah MF, Azmi AS, Ahmad A, Shamim U, Zubair H, Khan HY. Pharmaceutical research. 2010; 27:979–988. [PubMed: 20119749]
22. Schmitt SM, Frezza M, Dou QP. Frontiers in bioscience. 2012; 4:375–391.
23. Cater MA, Pearson HB, Wolyniec K, Klaver P, Bilandzic M, Paterson BM, Bush AI, Humbert PO, La Fontaine S, Donnelly PS, Haupt Y. ACS chemical biology. 2013; 8:1621–1631. [PubMed: 23656859]
24. Neyrolles O, Wolschendorf F, Mitra A, Niederweis M. Immunological reviews. 2015; 264:249–263. [PubMed: 25703564]
25. Djoko KY, Goytia MM, Donnelly PS, Schembri MA, Shafer WM, McEwan AG. Antimicrobial agents and chemotherapy. 2015
26. O'Boyle NM, Banck M, James CA, Morley C, Vandermeersch T, Hutchison GR. J Cheminform. 2011; 3:33. [PubMed: 21982300]
27. Speer A, Shrestha TB, Bossmann SH, Basaraba RJ, Harber GJ, Michalek SM, Niederweis M, Kutsch O, Wolschendorf F. Antimicrobial agents and chemotherapy. 2013; 57:1089–1091. [PubMed: 23254420]
28. Lech T, Sadlik JK. Biological trace element research. 2007; 118:16–20. [PubMed: 17848726]
29. Benesi HA, Hildebrand JH. Journal of the American Chemical Society. 1949; 71:2703–2707.
30. Bento AP, Gaulton A, Hersey A, Bellis LJ, Chambers J, Davies M, Krüger FA, Light Y, Mak L, McGlinchey S, Nowotka M, Papadatos G, Santos R, Overington JP. Nucleic acids research. 2014; 42:D1083–D1090. [PubMed: 24214965]
31. Davies M, Nowotka M, Papadatos G, Atkinson F, van Westen G, Dedman N, Ochoa R, Overington J. Challenges. 2014; 5:334.
32. Lisher JP, Giedroc DP. Frontiers in cellular and infection microbiology. 2013; 3:91. [PubMed: 24367765]
33. Goudouri OM, Kontonasaki E, Lohbauer U, Boccaccini AR. Acta biomaterialia. 2014; 10:3795–3810. [PubMed: 24704700]
34. Lipinski CA. Drug Discovery Today: Technologies. 2004; 1:337–341. [PubMed: 24981612]
35. Keller TH, Pichota A, Yin Z. Current opinion in chemical biology. 2006; 10:357–361. [PubMed: 16814592]

36. Liu J, Obando D, Liao V, Lifa T, Codd R. *European journal of medicinal chemistry*. 2011; 46:1949–1963. [PubMed: 21354674]
37. Smith, GF. *Progress in Medicinal Chemistry*. Lawton, G.; Witty, DR., editors. Vol. 50. Elsevier; 2011. p. 1-47.
38. Petersen HJ, Nielsen CK, Arrigoni-Martelli E. *Journal of medicinal chemistry*. 1978; 21:773–781. [PubMed: 691003]
39. Högberg M, Engelhardt P, Vrang L, Zhang H. *Bioorganic & medicinal chemistry letters*. 2000; 10:265–268. [PubMed: 10698450]
40. Hassan GS, El-Messery SM, Al-Omary FAM, Al-Rashood ST, Shabayek MI, Abulfadl YS, Habib E-SE, El-Hallouty SM, Fayad W, Mohamed KM, El-Menshawi BS, El-Subbagh HI. *European journal of medicinal chemistry*. 2013; 66:135–145. [PubMed: 23792351]
41. Irving H, Williams RJP. *Journal of the Chemical Society (Resumed)*. 1953:3192–3210.
42. Nies, D. *Molecular Microbiology of Heavy Metals*. Nies, D.; Silver, S., editors. Vol. 6. Springer Berlin Heidelberg; 2007. p. 117-142.
43. Macomber L, Imlay JA. *Proc Natl Acad Sci USA*. 2009; 106:8344–8349. [PubMed: 19416816]
44. Johnson MDL, Kehl-Fie TE, Rosch JW. *Metallomics : integrated biometal science*. 2015
45. Djoko KY, McEwan AG. *ACS chemical biology*. 2013; 8:2217–2223. [PubMed: 23895035]
46. Strebhardt K, Ullrich A. *Nature reviews. Cancer*. 2008; 8:473–480.
47. Djoko KY, Goytia MM, Donnelly PS, Schembri MA, Shafer WM, McEwan AG. *Antimicrobial agents and chemotherapy*. 2015; 59:6444–6453. [PubMed: 26239980]
48. Grass G, Rensing C, Solioz M. *Applied and environmental microbiology*. 2011; 77:1541–1547. [PubMed: 21193661]
49. Liu X, Li X, Zhang Z, Dong Y, Liu P, Zhang C. *Biological trace element research*. 2013; 154:150–155. [PubMed: 23716177]
50. Cooper GJ. *Drugs*. 2011; 71:1281–1320. [PubMed: 21770477]
51. Macomber L, Rensing C, Imlay JA. *Journal of bacteriology*. 2007; 189:1616–1626. [PubMed: 17189367]
52. Rensing C, Grass G. *FEMS microbiology reviews*. 2003; 27:197–213. [PubMed: 12829268]
53. Szymanski P, Fraczek T, Markowicz M, Mikiciuk-Olasik E. *Biometals : an international journal on the role of metal ions in biology, biochemistry, and medicine*. 2012; 25:1089–1112.
54. Beeton ML, Aldrich-Wright JR, Bolhuis A. *Journal of inorganic biochemistry*. 2014; 140:167–172. [PubMed: 25124857]
55. Bottari B, Maccari R, Monforte F, Ottana R, Rotondo E, Vigorita MG. *Bioorganic & medicinal chemistry letters*. 2000; 10:657–660. [PubMed: 10762047]
56. Chohan ZH, Arif M, Shafiq Z, Yaqub M, Supuran CT. *Journal of enzyme inhibition and medicinal chemistry*. 2006; 21:95–103. [PubMed: 16570512]
57. Chohan ZH, Pervez H, Rauf A, Scozzafava A, Supuran CT. *Journal of enzyme inhibition and medicinal chemistry*. 2002; 17:117–122. [PubMed: 12420758]
58. Gershon H, Parmegianir, Nickerson WJ. *Applied microbiology*. 1962; 10:556–560. [PubMed: 13960593]
59. Ming LJ, Epperson JD. *Journal of inorganic biochemistry*. 2002; 91:46–58. [PubMed: 12121761]

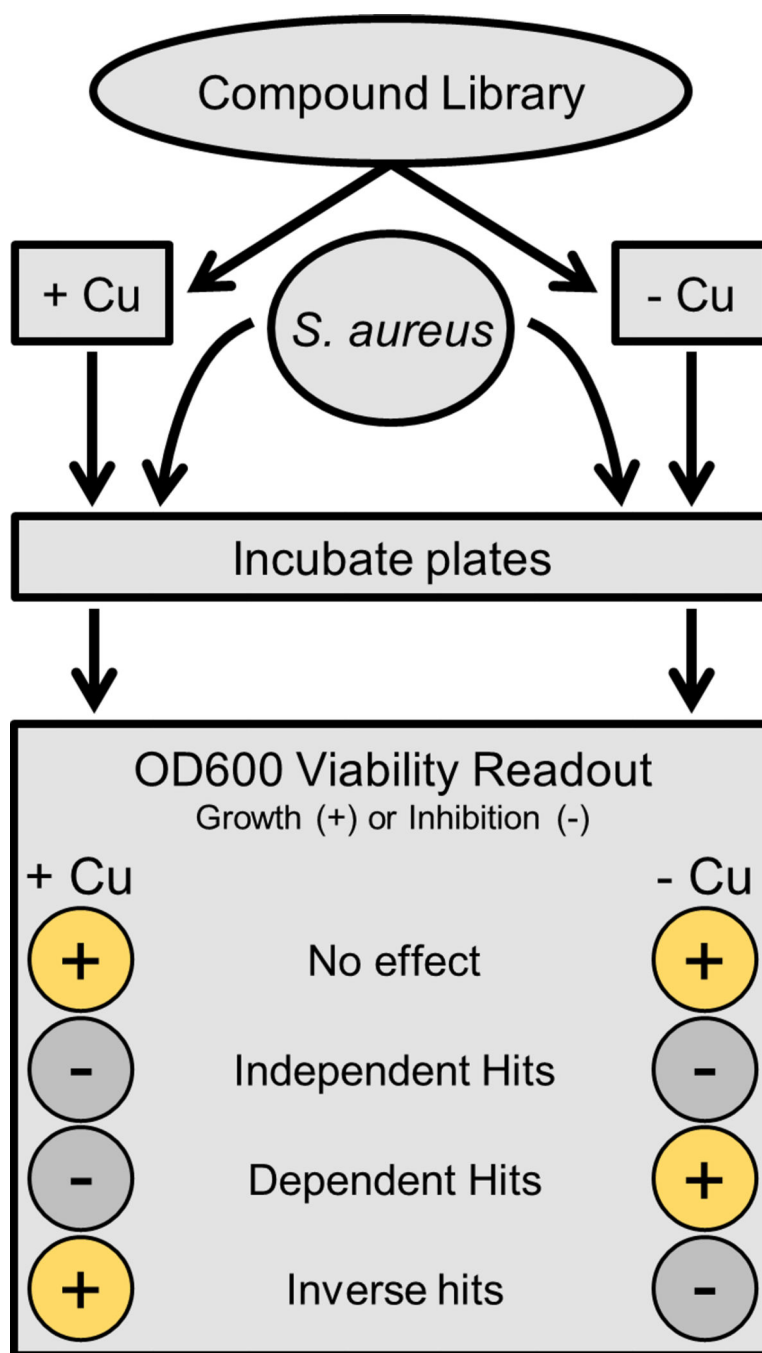


**Figure 1. Parallel combinatorial scheme**

Compounds from a master library are assayed twice in parallel, with one plate containing added copper sulfate, and the other containing only base medium. After adding *S. aureus*, both plates are incubated and viability is determined via OD600. Hits were classified by comparing growth values in both plates; the specific criteria used are detailed in the Materials and Methods.

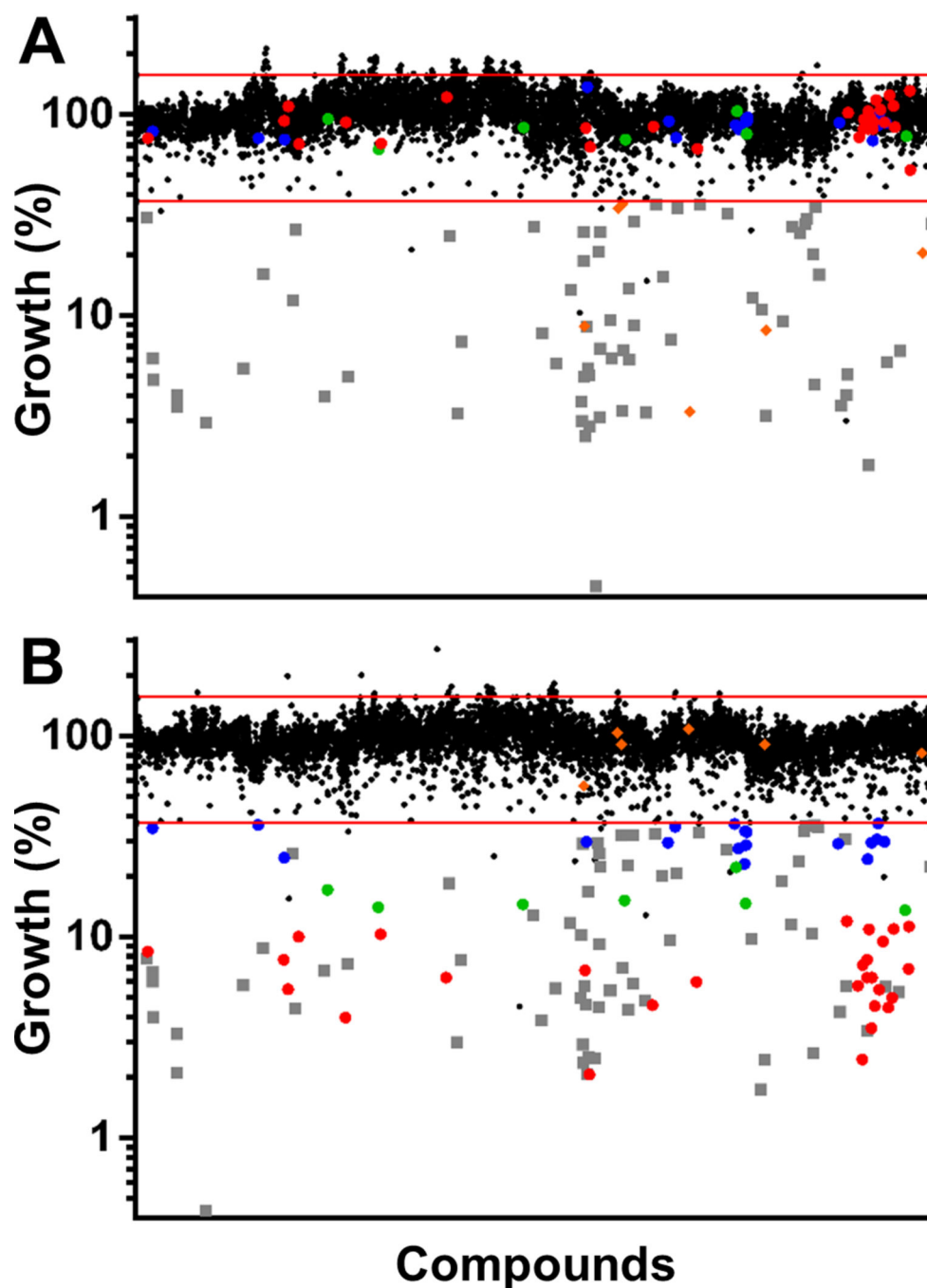


**Figure 2. Combinatorial screening results**

(A) Growth values of all 10,000 compounds in standard screening medium as normalized to plate controls. The red lines represent three standard deviations above and below the mean growth value as a cutoff for hits. (B) Growth values of all compounds in medium with copper added, as normalized to plate controls. Red, green, and blue circles are Primary (growth  $\leq 10\%$ , and greater than 2 SD below the  $-Cu$  plate), Secondary ( $10\% > \text{growth} \geq 20\%$ , and greater than 2 SD below the  $-Cu$  plate), and Tertiary ( $20\% > \text{growth} \geq 34\%$ , and greater than 2 SD below the  $-Cu$  plate) dependent hits; grey boxes are independent hits; and

orange diamonds are inverse hits. Some outliers may have fallen below the lower cut-off line but were classified as inactive because they did not meet hit criteria.

Author Manuscript

Author Manuscript

Author Manuscript

Author Manuscript

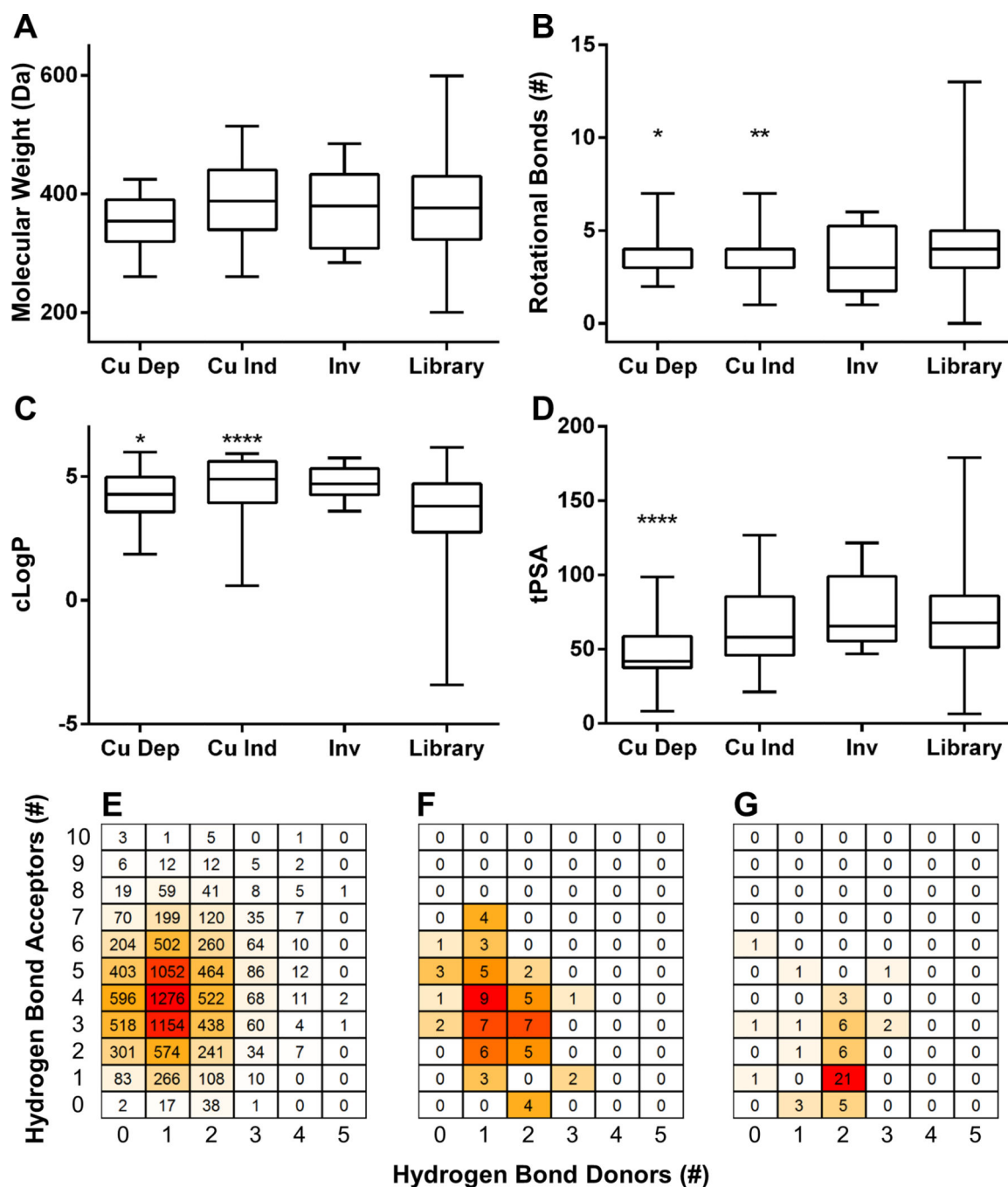


**Figure 3. Lipinski Rule of Five characteristics**

Aggregate (A) molecular weight, (B) rotational bonds, (C) calculated LogP (cLogP), and (D) topological polar surface area (tPSA) properties of copper-dependent hits (Cu Dep), copper-independent hits (Cu Ind), and inverse hits (Inv). All groups were compared to the screened library as a whole (Library) using a one way ANOVA and Dunnett's multiple comparisons test. \*  $p < 0.05$ , \*\*  $p < 0.01$ , \*\*\*\*  $p < 0.0001$ . (E) Heatmap comparisons of the hydrogen bond acceptors and donors within the entire screened library, (F) copper-independent hits, and (G) copper-dependent hits.



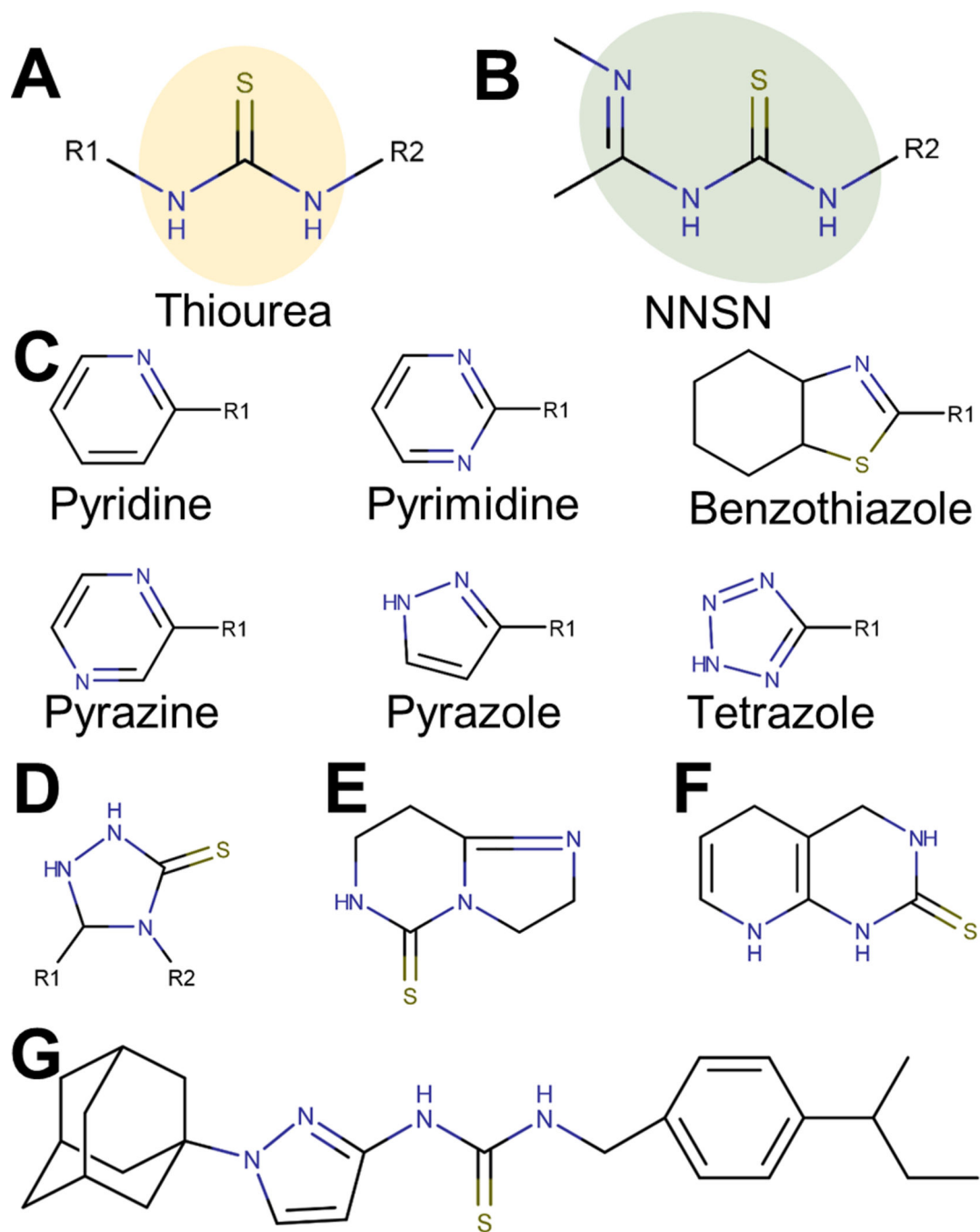
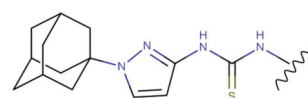


**Figure 4. A novel copper-binding NNSN motif and side groups**  
 47 copper-dependent hits contained a thiourea (A), with 12 featuring an extended NNSN motif (B) that consists of the thiourea base group paired with one of 6 possible heterocyclic nitrogen-containing ring structures (C). Compounds with a rigid and inflexible NNSN motif (D, E, F) conferred no activity. (G) Full structure of APT-6i.



Structure	MIC
6a	10
6b	5-10
6c	5-10
6d	5-10
6e	2.5
6f	2.5
6g	1.25
6h	0.6
6i	0.3

**Figure 5. Structure activity relationship analysis**

Nine analogs of a promising hit molecule were purchased from the supplier (ChemBridge) and examined for antimicrobial activity.

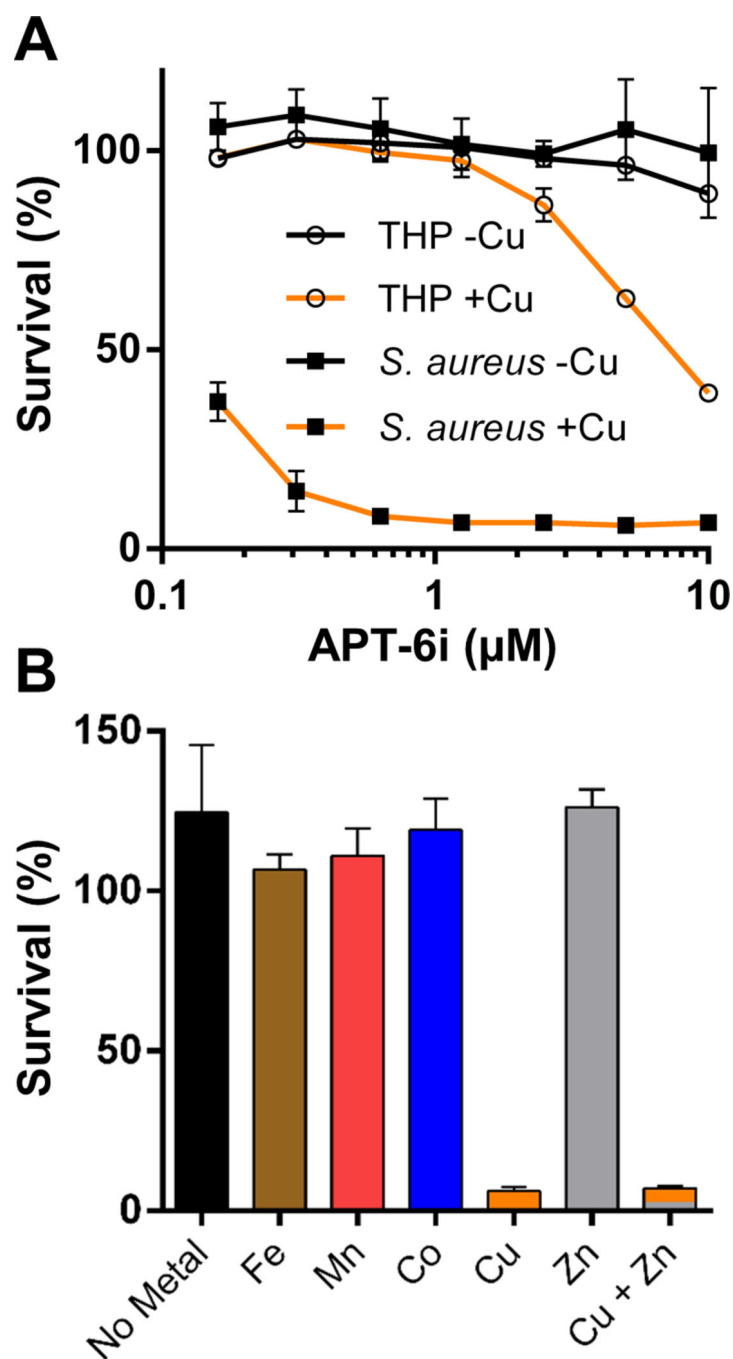


**Figure 6. APT-6i exhibits stark copper dependency and specificity**

(A) Inhibitory effects of APT-6i against *S. aureus* (black squares) and THP-1 cells, a human monocyte line (open circles). APT-6i is active only in the presence of copper (orange line). (B) Activity of 10 μM APT-6i against *S. aureus* grown in RPMI to better resolve metal dependencies. Cu is included at 50 μM, and Fe, Mn, Co, and Zn are included at 100 μM. Inhibition is strictly copper-specific, and occurs in the presence of other ions, such as a Cu/Zn coinubation. All values are normalized to the respective 0 μM compound control (either with or without copper), and expressed as percentages of survival.

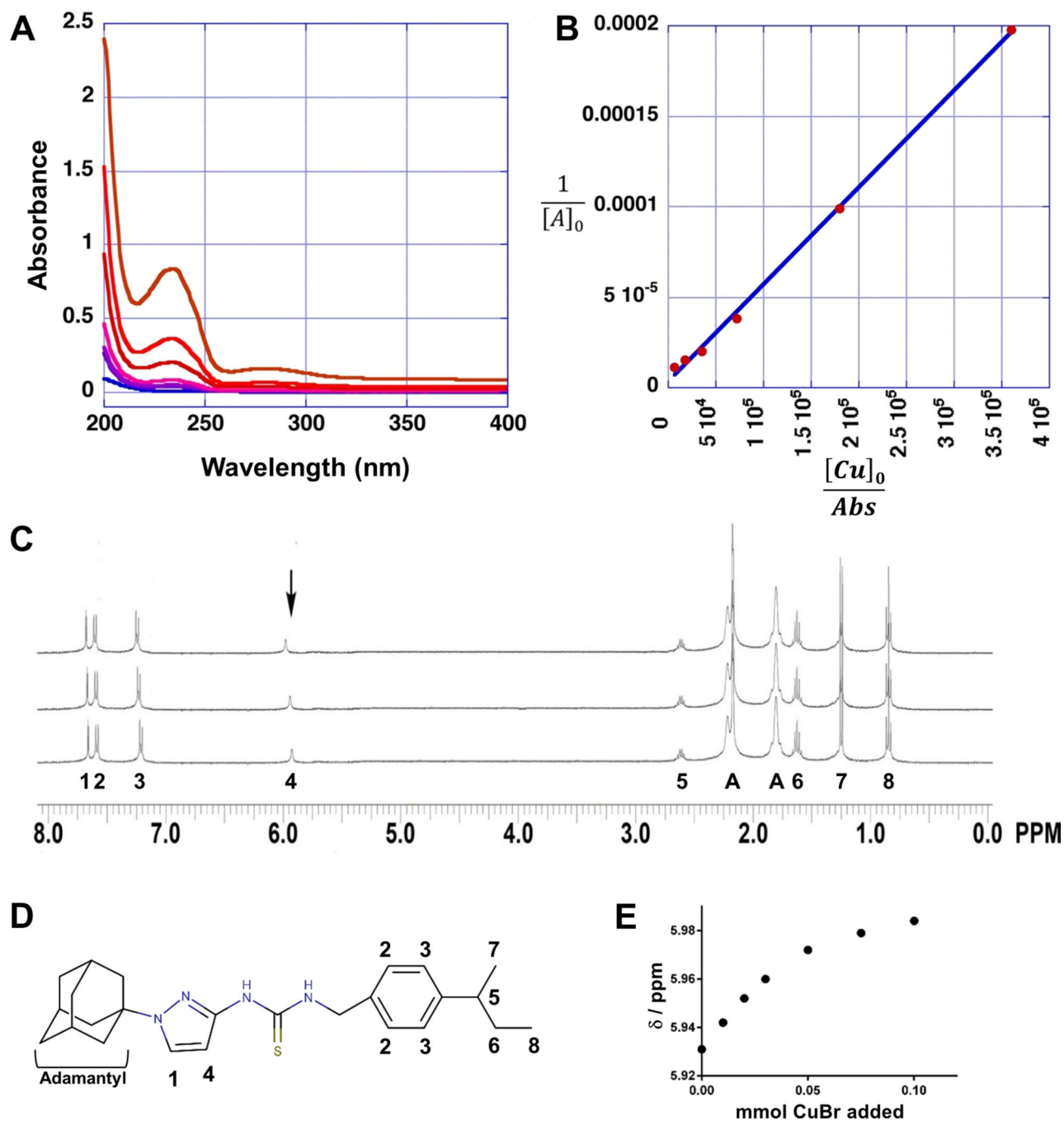


**Figure 7. APT-6i forms a unique copper complex**

(A) UV/Vis absorption spectra of compound APT-6i in the presence of 3.3  $\mu\text{M}$  Cu(I)Br in Trizma-HCl (pH=7)/methanol (90/10 v/v). Concentrations of APT-6i were 8.3 nM, 17 nM, 41 nM, 83 nM, 170 nM and 410 nM. (B) Benesi Hildebrand plots for determining the binding constant and molar absorption coefficients of APT-6i with CuBr. (C) Overlay of the  $^1\text{H}$ -NMR spectra (Bruker Avance III, 600 MHz, 298K) of compound APT-6i without CuBr (bottom), with 50  $\mu\text{M}$  CuBr (middle), and with 100  $\mu\text{M}$  CuBr (top) in deuterated acetone. Peak assignments correspond to panel D with A=adamantyl. The arrow indicates a

copper responsive peak shift. (D) Structure of APT-6i showing relevant peak assignments and match with panel C. (E) Shift of highlighted peak 4 with increasing concentrations of CuBr from panel C, indicating an interaction with copper ions at these sites.

Author Manuscript

Author Manuscript

Author Manuscript

Author Manuscript

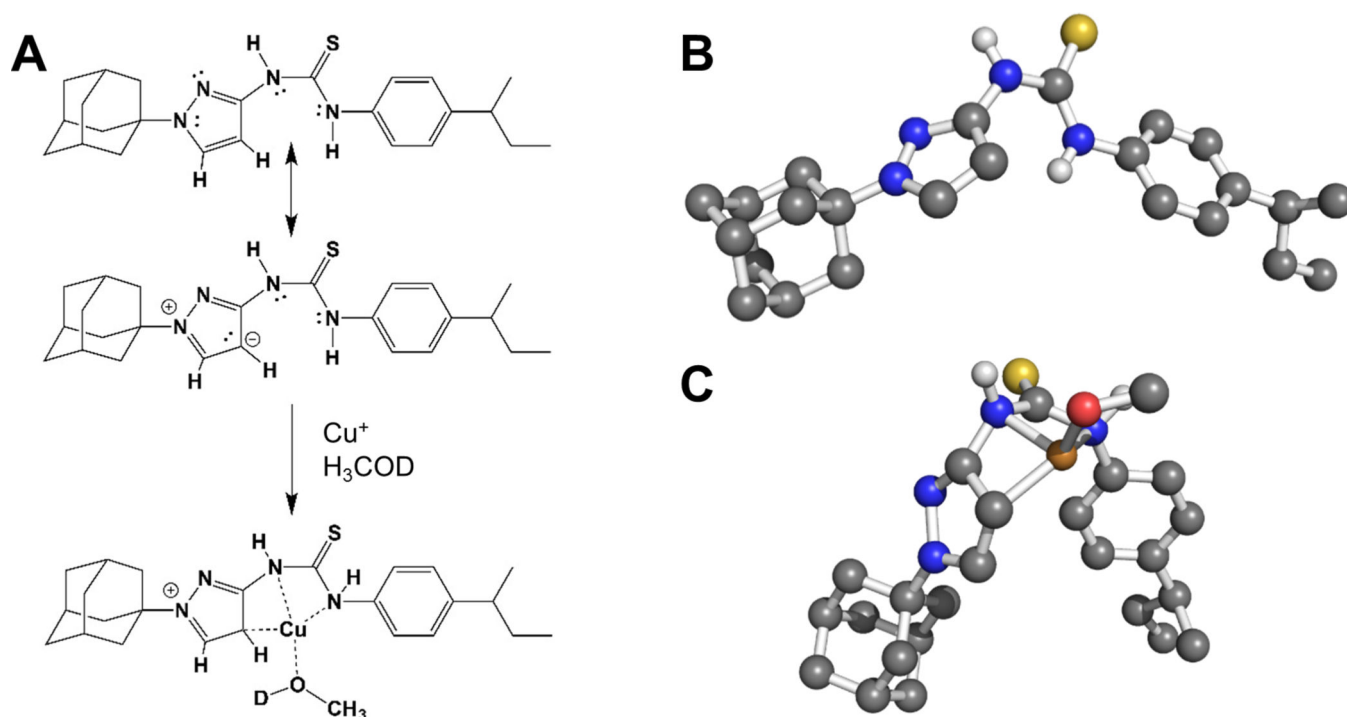


**Figure 8. The APT-6i and copper complex has unique coordination chemistry**

The complex's geometry was determined using UV-Vis and  $^1\text{H-NMR}$ , shown in Figure 7.

(A) The (minor) resonance structure of APT-6i is able to form a complex with  $\text{Cu(I)}$ . (B) 3D representation of uncomplexed APT-6i using the CHARMM force field, showing a relatively linear structure. Non-polar hydrogens are removed for clarity. (C) 3D model of the APT-6i/ $\text{Cu(I)}$ / $\text{CH}_3\text{OD}$  complex. Coordination twists the molecule from a linear structure to a bent configuration. Copper is represented as the orange sphere, with a  $\text{D}_1$ -methanol added to the coordination complex. Yellow sphere represents sulfur, blue are nitrogen atoms, grey are carbon atoms and white are polar hydrogens.

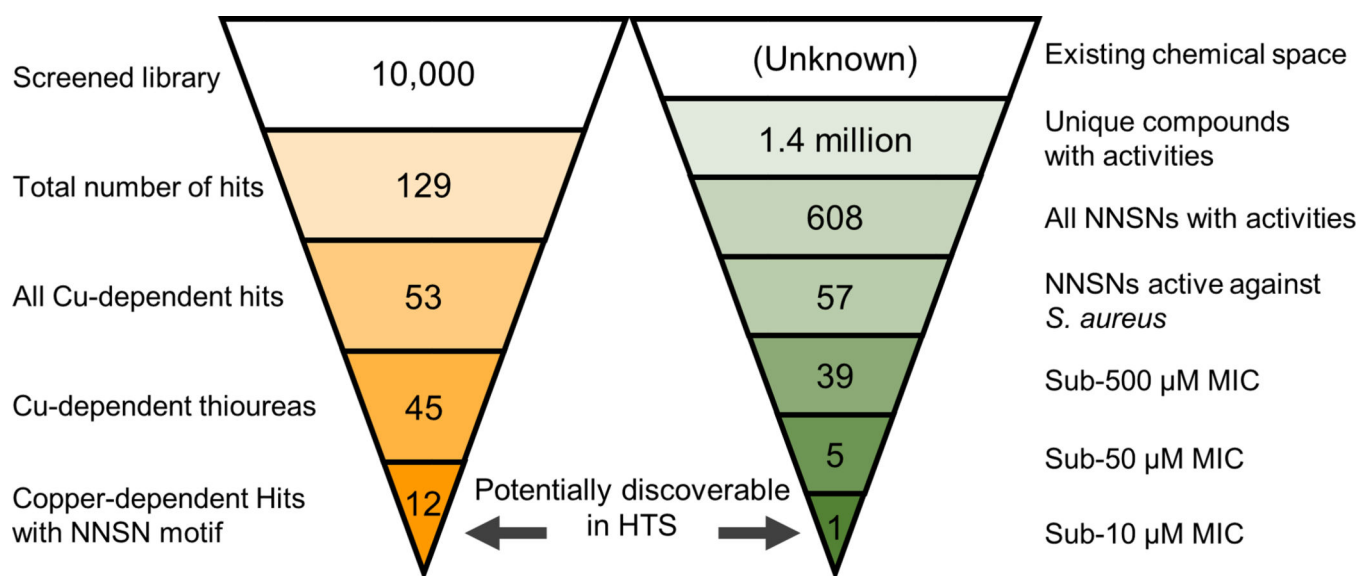


**Figure 9. Cheminformatic search of the ChEMBL database**

The ChEMBL cheminformatic database was queried with the NNSN motif for similar molecules. Though the limited screen described here revealed 12 NNSNs with significant antibacterial effects, only a single NNSN with activity against *S. aureus* below 10  $\mu\text{M}$  was found within the database.